Direction Finding/Polarization Estimation—Dipole and/or Loop Triad(s)

KAINAM THOMAS WONG, Senior Member, IEEE
Chinese University of Hong Kong

This paper shows 1) how measurement of the three Cartesian components of the electrical-field *or* magnetic-field suffices for multisource azimuth/elevation direction finding and polarization estimation, and 2) how the vector cross-product direction-of-arrival estimator is fully applicable even when the dipole triad is arbitrarily displaced from the loop triad.

Manuscript received June 1, 2000; revised October 24, 2000; released for publication December 21, 2000.

IEEE Log No. T-AES/37/2/06339.

Refereeing of this contribution was handled by Dr. Jim P. Y. Lee.

Part of this work was presented at the 1999 *IEEE International Conference on Circuits & Systems*.

This research work was supported by Direct Grants 2050187 and 1050247 and Mainline Grant 44M5010, all from Hong Kong's Research Grant Council.

Author's address: Department of Electronic Engineering, Chinese University of Hong Kong, Shatin, NT, Hong Kong, E-mail: (ktwong@ieee.org).

I. INTRODUCTION

A series of recent papers, [3–12, 14–18, 20, 21] among others, investigates the use of collocated six-component electromagnetic vector sensors for diversely polarized direction-of-arrival (DOA) estimation. A collocated six-component vector sensor consists of three identical and collocated but orthogonally oriented electrically short dipoles (called a dipole triad) plus three identical collocated but orthogonally oriented magnetically small loops (called a loop triad). All six component-antennas are spatially collocated in a point-like geometry. The collocated six-component vector sensor offers the following advantages: 1) the polarization diversity among the vector sensor's component antennas allows that incident sources to be separated on account of their polarization differences in addition to their azimuth/elevation angular differences; 2) the spatial collocation of all component antennas in the vector sensor means no *spatial* phase delay in the vector sensor steering vector; hence, near-field sources may be located by an individual vector sensor as well as far-field sources; and 3) in a multisource scenario, each source's three Cartesian direction cosine estimates (and thus each source's azimuth angle estimate and the elevation angle estimate) are automatically paired without further post-processing. Theoretical performance bounds for direction finding using the collocated six-component vector sensors have been defined and derived in [3, 5].

A variety of eigenstructure-based direction finding, polarization estimation and tracking schemes [6–12, 14–18, 20, 21] have deployed these collocated six-component vector sensors in diverse array configurations for various signal scenarios using the vector cross-product DOA estimator. This vector cross-product DOA estimator exploits all six Cartesian components of the incident electromagnetic field to estimate the kth source's amplitude-normalized Poynting vector $\mathbf{p}_k$, which, in turn, gives estimates of the source's elevation angle θ_k (measured from the positive z-axis) and the azimuth angle ϕ_k (measured from the positive x-axis):

$$\mathbf{p}_k \stackrel{\text{def}}{=} \begin{bmatrix} p_{x_k} \\ p_{y_k} \\ p_{z_k} \end{bmatrix} = \frac{\mathbf{e}_k \times \mathbf{h}_k^*}{\|\mathbf{e}_k\| \quad \|\mathbf{h}_k^*\|} \stackrel{\text{def}}{=} \begin{bmatrix} u_k \\ v_k \\ w_k \end{bmatrix} = \begin{bmatrix} \sin\theta_k & \cos\phi_k \\ \sin\theta_k & \sin\phi_k \\ \cos\theta_k & \end{bmatrix} \tag{1}$$

where $*$ denotes complex conjugation, $\mathbf{e}_k$ and $\mathbf{h}_k$, respectively, denote the kth source's electric-field vector and magnetic-field vector, u_k, v_k, and w_k, respectively, represent the kth source's direction-cosines along the x-axis, the y-axis, and the z-axis. This vector cross-product DOA estimation approach complements the customary interferometry direction finding approach, which estimates the spatial phase delay among the data sets collected at physically displaced antennas.

The six-component electromagnetic vector-sensor, however, suffers from mutual coupling between its dipole triad and its loop triad. If only one triad (but not both) is deployed or if some significant distance separates the two triads, then the above mentioned coupling problem may be mitigated. Moreover deploying only one triad reduces antenna and receiver electronic hardware costs, simplifies algorithmic complexity, completely avoids the inter-dipole/loop triad mutual coupling problem, and eliminates the need to synchronize the phase between the dipole triad and the loop triad.

This work shows 1) how a *dipole* triad by itself suffices for multisource azimuth/elevation direction finding and polarization estimation, 2) how a *loop* triad by itself suffices for multisource azimuth/elevation direction finding and polarization estimation, and 3) how the vector cross-product DOA estimator remains fully applicable for a pair of dipole triad and loop triad spatially displaced by an arbitrary and (possibly) unknown distance (rather than being collocated). The above contrasts with the case of a collocated pair of perpendicularly oriented dipoles (commonly used in mobile communications), which is insufficient for exact estimation of the sources' arrival angles. In [19], however, it is shown that two horizontally oriented and magnetically small loops (plus an optional vertically oriented short dipole) can *approximately* estimate the sources' azimuth angles. Such an antenna array set-up matches the polarization of the wireless handset transmitter's strong vertical electric-field and can be used to retrofit dumb antenna-array receivers at the cellular base-station for downlink transmission beamforming.

II. MATHEMATICAL MODELS OF STEERING VECTORS

The kth unit-power completely polarized[1] transverse electromagnetic wave, having traveled through a homogeneous isotropic medium, is characterized by the electric-field vector $\mathbf{e}_k$ and the magnetic-field vector $\mathbf{h}_k$, expressible in Cartesian coordinates as [3, 4]:

$$\begin{bmatrix}\mathbf{e}_k\\ \mathbf{h}_k\end{bmatrix} \stackrel{\text{def}}{=} \begin{bmatrix} e_x(\theta_k,\phi_k,\gamma_k,\eta_k)\\ e_y(\theta_k,\phi_k,\gamma_k,\eta_k)\\ e_z(\theta_k,\gamma_k,\eta_k)\\ h_x(\theta_k,\phi_k,\gamma_k,\eta_k)\\ h_y(\theta_k,\phi_k,\gamma_k,\eta_k)\\ h_z(\theta_k,\gamma_k)\end{bmatrix}$$

$$\stackrel{\text{def}}{=} \underbrace{\begin{bmatrix} \cos\phi_k\cos\theta_k & -\sin\phi_k\\ \sin\phi_k\cos\theta_k & \cos\phi_k\\ -\sin\theta_k & 0\\ -\sin\phi_k & -\cos\phi_k\cos\theta_k\\ \cos\phi_k & -\sin\phi_k\cos\theta_k\\ 0 & \sin\theta_k \end{bmatrix}}_{\stackrel{\text{def}}{=}\boldsymbol{\Theta}(\theta_k,\phi_k)} \underbrace{\begin{bmatrix}\sin\gamma_k e^{j\eta_k}\\ \cos\gamma_k\end{bmatrix}}_{\stackrel{\text{def}}{=}\mathbf{g}_k} \qquad (2)$$

where $0 \le \theta_k < \pi/2$ denotes the signal's elevation angle measured from the vertical z-axis, $0 \le \phi_k < 2\pi$ symbolizes the azimuth angle measured from the positive x-axis, $0 \le \gamma_k < \pi/2$ refers to the auxiliary polarization angle, and $-\pi \le \eta_k < \pi$ represents the polarization phase difference. Note that $\boldsymbol{\Theta}(\theta_k,\phi_k)$ depends only on the angular parameters, whereas $\mathbf{g}_k$ depends only on the polarizational parameters. Also, $\|\mathbf{e}_k\| = \|\mathbf{h}_k\| = 1$ for all values of $(\theta_k,\phi_k,\gamma_k,\eta_k)$.

The dipole triad has the steering vector $\mathbf{a}_k = \mathbf{e}_k$. The loop triad has the steering vector $\mathbf{a}_k = \mathbf{h}_k$. A dipole triad plus a displaced but identically oriented loop triad (with the loop triad located at (d_x,d_y,d_z) relative to the dipole triad) has the steering vector

$$\mathbf{a}_k = \begin{bmatrix}\mathbf{e}_k\\ \mathbf{h}_k q_H(u_k,v_k)\end{bmatrix},$$

where $q_H(u_k,v_k)$ is defined as $e^{j2\pi(d_x u_k + d_y v_k + d_z w_k)/\lambda}$ and represents the *spatial* phase-factor relating the measurement at the loop triad to that at the dipole triad. λ denotes the signals' wavelength. For reference,

$$\mathbf{a}_k = \begin{bmatrix}\mathbf{e}_k\\ \mathbf{h}_k\end{bmatrix}$$

for the collocated six-component vector sensor.

The dipole triad, the loop triad, or the dipole-triad-plus-loop-triad displaced pair may be used as a multicomponent element in a multielement array for direction finding and polarization estimation, just as the collocated six-component vector sensor has been used in [3–12, 14–18, 20, 21]. Specifically, in [8] a single collocated six-component vector sensor (along with a *temporal-invariance* version of ESPRIT[2]) to estimate the arrival angles and polarization states of multiple pure tones, while in [10, 21] the same is done for multiple frequency-hop (FH) signals. In [6, 7, 17, 18] a number of collocated six-component vector sensors are employed in a sparse (thinned) $L \times M$ rectangular array without incurring any cyclic ambiguity in the final estimates of the sources' Cartesian direction cosines by the use of a *spatial-invariance* version of ESPRIT. In

[1]Partially polarized or unpolarized sources may be handled using the techniques presented in [12].

[2]ESPRIT [2] is a closed-form eigenstructure-based parameter estimation technique that requires the data to possess certain "invariance" structures.

[9, 20], arbitrarily and irregularly spaced three-dimensional arrays of collocated six-component vector sensors are proposed in conjunction with a MUSIC[3]-based algorithm that needs no initial coarse estimates to start off MUSIC's iterative search. In [11, 16], it is shown how the above arbitrarily spaced collocated six-component vector sensors are handled, using a *polarization-invariance* version of ESPRIT, when their locations are unknown. In all above mentioned schemes, the collocated six-component vector sensor may be substituted by the dipole triad, or the loop triad, or the dipole-triad-plus-loop-triad displaced pair; and this paper shows how. Without reciting the algorithmic details, all aforementioned schemes involve eigenstructure-based parameter estimation algorithmic steps that lead to an estimate of each incident source's steering vector, correct to within an *unknown* complex-value scalar c_k. That is, available somewhere in each algorithm is the estimate $\hat{\mathbf{a}}_k \approx c_k \mathbf{a}_k$. (The approximation becomes a straight equality in noiseless or asymptotic cases.) The question is whether $\hat{\mathbf{a}}_k$ suffices to unambiguously estimate the kth source's arrival angles and polarization states when $\mathbf{a}_k$ corresponds to the steering vector of a dipole triad, a loop triad, or a dipole-triad-plus-loop-triad displaced pair. The answer is "yes" and the following section shows how.

III. ESTIMATION FORMULAS FOR THE ARRIVAL ANGLES AND POLARIZATION PARAMETERS

The key observation is that $\|\mathbf{e}_k\| = \|\mathbf{h}_k\| = \|\mathbf{p}_k\| = 1$ for all $(\theta_k, \phi_k, \gamma_k, \eta_k)$. This means that the uncertainty in $\hat{\mathbf{a}}_k$ due to $|c_k|$ may be removed by amplitude-normalizing $\hat{\mathbf{a}}_k$ in the cases of the dipole triad and the loop triad to produce a unity Frobenius norm. Algebraic and trigonometric manipulations on this normalized $\hat{\mathbf{a}}_k/\|\hat{\mathbf{a}}_k\|$ then produce five real-valued nonlinear equations, leading to unambiguous estimation of $\{\theta_k, \phi_k, \gamma_k, \eta_k\}$.

A. For Dipole Triad

If dipole triads are deployed, $\hat{\mathbf{a}}_k = c_k \mathbf{e}_k$ under noiseless or asymptotic conditions. Hence,

$$\frac{\hat{\mathbf{a}}_k e^{-j\angle[\hat{\mathbf{a}}_k]_3}}{\|\hat{\mathbf{a}}_k\|} = \begin{bmatrix} -\cos\theta_k\cos\phi_k\sin\gamma_k + \cos\gamma_k\sin\phi_k\cos\eta_k \\ -\cos\theta_k\sin\phi_k\sin\gamma_k - \cos\gamma_k\cos\phi_k\cos\eta_k \\ \sin\theta_k\sin\gamma_k \end{bmatrix} + j\begin{bmatrix} -\cos\gamma_k\sin\phi_k\sin\eta_k \\ \cos\gamma_k\cos\phi_k\sin\eta_k \\ 0 \end{bmatrix} \quad (3)$$

where $[\cdot]_i$ refers to the ith element in the bracketed vector and $\angle$ denotes the angle of the ensuing entity. The above array manifold model has not accounted for the dipoles' mutual coupling effects; however, good isolation and balance among the dipoles can minimize intratriad mutual coupling and renders the above array manifold model a very realistic approximation The above expression shows that the real and imaginary parts of $e^{-j\angle[\hat{\mathbf{a}}_k]_3}\hat{\mathbf{a}}_k/\|\hat{\mathbf{a}}_k\|$, as five real-valued separate entities, producing for each incident source five separate nonlinear real-valued equations relating the four unknown signal parameters $\{\theta_k, \phi_k, \gamma_k, \eta_k\}$. Manipulation of these equations gives

$$\hat{\phi}_k = \begin{cases} \tan^{-1}\dfrac{-\mathrm{Im}\{[\hat{\mathbf{a}}_k e^{-j\angle[\hat{\mathbf{a}}_k]_3}]_1\}}{\mathrm{Im}\{[\hat{\mathbf{a}}_k e^{-j\angle[\hat{\mathbf{a}}_k]_3}]_2\}}, & \text{if } \mathrm{Im}\{[\hat{\mathbf{a}}_k e^{-j\angle[\hat{\mathbf{a}}_k]_3}]_1\} < 0 \\ \tan^{-1}\dfrac{-\mathrm{Im}\{[\hat{\mathbf{a}}_k e^{-j\angle[\hat{\mathbf{a}}_k]_3}]_1\}}{\mathrm{Im}\{[\hat{\mathbf{a}}_k e^{-j\angle[\hat{\mathbf{a}}_k]_3}]_2\}} + \pi, & \text{if } \mathrm{Im}\{[\hat{\mathbf{a}}_k e^{-j\angle[\hat{\mathbf{a}}_k]_3}]_1\} \geq 0 \end{cases} \quad (4)$$

$$\hat{\theta}_k = \tan^{-1}\left\{\left\|\frac{[\hat{\mathbf{a}}_k]_3}{\mathrm{Re}\{[\hat{\mathbf{a}}_k]_1 e^{-j\angle[\hat{\mathbf{a}}_k]_3}\}\cos\hat{\phi}_k + \mathrm{Re}\{[\hat{\mathbf{a}}_k]_2 e^{-j\angle[\hat{\mathbf{a}}_k]_3}\}\sin\hat{\phi}_k}\right\|\right\} \quad (5)$$

$$\hat{\gamma}_k = \sin^{-1}\left\{\frac{\|[\hat{\mathbf{a}}_k]_3\|}{\sin\hat{\theta}_k}\right\} \quad (6)$$

$$\hat{\eta}_k = [\hat{\mathbf{a}}_k e^{-j\angle[\hat{\mathbf{a}}_k]_3}]_1 \sin\hat{\phi}_k + [\hat{\mathbf{a}}_k e^{-j\angle[\hat{\mathbf{a}}_k]_3}]_2 \cos\hat{\phi}_k. \quad (7)$$

Thus, the unknown complex-valued scalar ambiguity c_k in $\hat{\mathbf{a}}_k$ needs to cause no ambiguity in the estimation of the arrival angles and polarization parameters.

B. For Loop Triad

If loop triads are deployed, $\hat{\mathbf{a}}_k = c_k \mathbf{h}_k$ under noiseless or asymptotic conditions. Hence,

$$\frac{\hat{\mathbf{a}}_k e^{-j\angle[\hat{\mathbf{a}}_k]_3}}{\|\hat{\mathbf{a}}_k\|} = \begin{bmatrix} -\cos\theta_k\cos\phi_k\cos\gamma_k + \sin\gamma_k\sin\phi_k\cos\eta_k \\ -\cos\theta_k\sin\phi_k\cos\gamma_k - \sin\gamma_k\cos\phi_k\cos\eta_k \\ \sin\theta_k\cos\gamma_k \end{bmatrix} + j\begin{bmatrix} -\sin\gamma_k\sin\phi_k\sin\eta_k \\ \sin\gamma_k\cos\phi_k\sin\eta_k \\ 0 \end{bmatrix}. \quad (8)$$

The above array manifold model has not accounted for the loops' mutual coupling effects; however, good isolation and balance among the loops can minimize intratriad mutual coupling and renders the above array manifold model a very realistic approximation. The z-axis component of $\mathbf{h}_k$ is always real in value regardless of the values of $(\theta, \phi, \gamma, \eta)$. With the left-hand-side of (8) already available, (8) produces for each incident source five nonlinear real-valued equations relating the four unknown

[3]MUSIC [1] is an iterative eigenstructure-based parameter estimation technique.

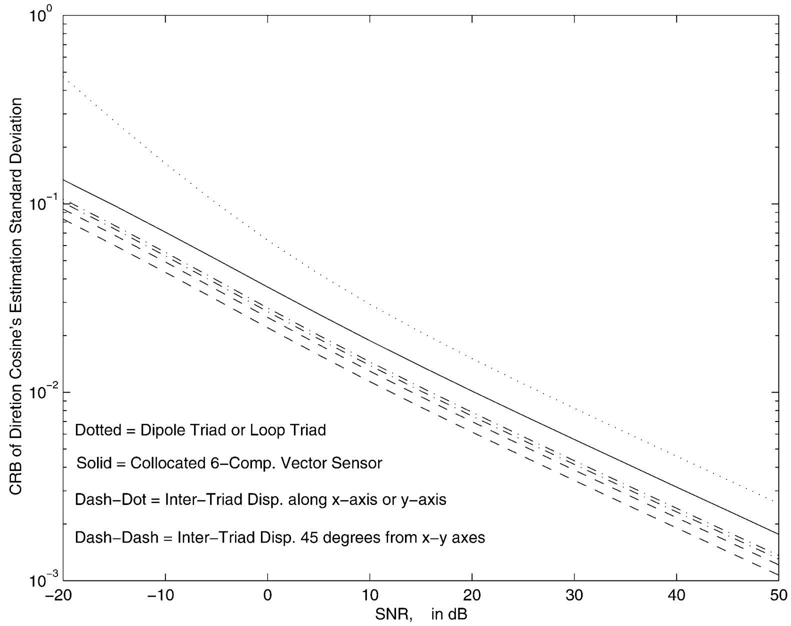

Fig. 1. CRBs for various multicomponent antennas versus SNR. There are two incident narrowband completely polarized uncorrelated sources with $(u_1, v_1, \eta_1, \gamma_1) = (0.41, 0.31, \pi/2, \pi/4)$ and $(u_2, v_2, \eta_2, \gamma_2) = (0.59, 0.49, -\pi/2, \pi/4)$. 200 snapshots used at each SNR value.

signal parameters. Manipulation of these equations gives

$$\hat{\phi}_k = \begin{cases} \tan^{-1}\dfrac{-\mathrm{Im}[\hat{\mathbf{a}}_k e^{-j\angle[\hat{\mathbf{a}}_k]_3}]_1}{\mathrm{Im}[\hat{\mathbf{a}}_k e^{-j\angle[\hat{\mathbf{a}}_k]_3}]_2}, & \text{if} \quad \mathrm{Im}[\hat{\mathbf{a}}_k e^{-j\angle[\hat{\mathbf{a}}_k]_3}]_1 < 0 \\ \tan^{-1}\dfrac{-\mathrm{Im}[\hat{\mathbf{a}}_k e^{-j\angle[\hat{\mathbf{a}}_k]_3}]_1}{\mathrm{Im}[\hat{\mathbf{a}}_k e^{-j\angle[\hat{\mathbf{a}}_k]_3}]_2} + \pi, & \text{if} \quad \mathrm{Im}[\hat{\mathbf{a}}_k e^{-j\angle[\hat{\mathbf{a}}_k]_3}]_1 \geq 0 \end{cases} \tag{9}$$

$$\hat{\theta}_k = \tan^{-1}\left\{\left\|\frac{\mathrm{Re}\{[\hat{\mathbf{a}}_k e^{-j\angle[\hat{\mathbf{a}}_k]_3}]_3\}}{\mathrm{Re}\{[\hat{\mathbf{a}}_k e^{-j\angle[\hat{\mathbf{a}}_k]_3}]_1\}\cos\hat{\phi}_k + \mathrm{Re}\{[\hat{\mathbf{a}}_k e^{-j\angle[\hat{\mathbf{a}}_k]_3}]_2\}\sin\hat{\phi}_k}\right\|\right\} \tag{10}$$

$$\hat{\gamma}_k = \cos^{-1}\left\{\frac{\mathrm{Re}\{[\hat{\mathbf{a}}_k]_3\}}{\sin\hat{\theta}_k}\right\} \tag{11}$$

$$\begin{aligned}\hat{\eta}_k = \angle\{&[\hat{\mathbf{a}}_k e^{-j\angle[\hat{\mathbf{a}}_k]_3}]_1 + \cos\hat{\phi}\cos\hat{\theta}_k\cos\hat{\gamma}_k \\ &+ [\hat{\mathbf{a}}_k e^{-j\angle[\hat{\mathbf{a}}_k]_3}]_2 + \sin\hat{\phi}_k\cos\hat{\theta}_k\cos\hat{\gamma}_k\}.\end{aligned} \tag{12}$$

C. For Displaced Dipole-Triad-Plus-Loop-Triad Pair

Recalling that

$$\hat{\mathbf{a}}_k = c_k \begin{bmatrix} \mathbf{e}_k \\ q_H(u_k, v_k)\mathbf{h}_k \end{bmatrix}$$

under noiseless or asymptotic conditions and that $\|q_H(u_k, v_k)\| = 1$,

$$\frac{(c_k\hat{\mathbf{e}}_k) \times (c_k q_H(u_k, v_k)\hat{\mathbf{h}}_k)^*}{\|(c_k\hat{\mathbf{e}}_k) \times (c_k q_H(u_k, v_k)\hat{\mathbf{h}}_k)^*\|} = \underbrace{q_H(u_k, v_k)\mathbf{p}_k}_{\overset{\text{def}}{=}\tilde{\mathbf{p}}_k} \tag{13}$$

where $\times$ denotes the vector cross product. Hence,

$$\mathbf{p}_k = \tilde{\mathbf{p}}_k e^{-j\angle[\tilde{\mathbf{p}}_k]_3} = \begin{bmatrix} u_k \\ v_k \\ w_k \end{bmatrix} = \begin{bmatrix} \sin\theta_k & \cos\phi_k \\ \sin\theta_k & \sin\phi_k \\ \cos\theta_k & \end{bmatrix} \tag{14}$$

with

$$\tilde{\mathbf{p}}_k = \frac{[\mathbf{I}_3 \vdots \mathbf{0}_3]\hat{\mathbf{a}}_k \times [\mathbf{0}_3 \vdots \mathbf{I}_3]\hat{\mathbf{a}}_k}{\|[\mathbf{I}_3 \vdots \mathbf{0}_3]\hat{\mathbf{a}}_k \times [\mathbf{0}_3 \vdots \mathbf{I}_3]\hat{\mathbf{a}}_k\|} \tag{15}$$

where $\mathbf{I}_3$ symbolizes a 3×3 identity matrix, and $\mathbf{0}_3$ refers to a 3×3 zero matrix. Hence,

$$\hat{\theta}_k = \arcsin\left(\sqrt{[\hat{\mathbf{p}}_k]_1^2 + [\hat{\mathbf{p}}_k]_2^2}\right) = \arccos([\hat{\mathbf{p}}_k]_3) \tag{16}$$

$$\hat{\phi}_k = \arctan([\hat{\mathbf{p}}_k]_2/[\hat{\mathbf{p}}_k]_1) \tag{17}$$

$$\hat{\gamma}_k = \arctan\frac{[\hat{\mathbf{g}}_k]_1}{[\hat{\mathbf{g}}_k]_2} \tag{18}$$

$$\hat{\eta}_k = \angle[\hat{\mathbf{g}}_k]_1 - \angle[\hat{\mathbf{g}}_k]_2 \tag{19}$$

where

$$\hat{\mathbf{g}}_k \overset{\text{def}}{=} [\tilde{\mathbf{\Theta}}_k^H \tilde{\mathbf{\Theta}}_k]^{-1}\tilde{\mathbf{\Theta}}_k^H \hat{\mathbf{a}}_k \tag{20}$$

$$\tilde{\mathbf{\Theta}}_k \overset{\text{def}}{=} [\mathbf{I}_3 \vdots q_H(\sin\hat{\theta}_k\cos\hat{\phi}_k, \sin\hat{\theta}_k\sin\hat{\phi}_k)\mathbf{I}_3]\mathbf{\Theta}(\hat{\theta}_k, \hat{\phi}_k). \tag{21}$$

IV. COMPARATIVE CRAMER–RAO BOUND PERFORMANCE

Fig. 1 plots the Cramer–Rao bound (CRB) [3] versus the signal-to-noise ratio (SNR) for the several multicomponent antenna types discussed in this work under a scenario involving two closely spaced, completely polarized, narrowband, uncorrelated far-field sources under additive white Gaussian noise. The source parameters are with $(u_1, v_1, \eta_1, \gamma_1) = (0.41, 0.31, \pi/2, \pi/4)$ and $(u_2, v_2, \eta_2, \gamma_2) = (0.59, 0.49, -\pi/2, \pi/4)$. There are 200 snapshots used at each SNR value.

The dipole triad and the loop triad has an exactly identical CRB curve, which is 3 dB higher than that of the collocated six-component vector sensor. This is expected because the former has half the number of component-antennas as the latter. The dash-dot and dash curves all refer to the dipole-triad-plus-loop-triad displaced pair case, revealing the effects of the intertriad displacement axis' length and orientation. The two dash-dot curves and the top dash curve all correspond to an half-wavelength intertriad axis, whereas the bottom dash curve refers to a five-wavelength intertriad axis. The top dash-dot curve has the intertriad displacement aligned along the x-axis; the lower dash-dot has the intertriad displacement aligned along the y-axis; and the upper dash curve has the inter-triad displacement 45° from the x-y axes. It may be observed that a longer intertriad axis gives better estimates because of the larger geometric aperture that results. The axis orientation that optimizes estimation performance is the orientation onto which the incident sources project the farthest angular separation. In the present signal scenario, the 45° orientation (clockwise from the positive x-axis) gives the two sources a wider angular separation than when the intertriad axis is aligned either along the x-axis or along the y-axis.

REFERENCES

[1] Schmidt, R. O. (1986)
Multiple emitter location and signal parameter estimation.
IEEE Transactions on Antennas and Propagation, **34**, 3 (Mar. 1986), 276–280.

[2] Roy, R., and Kailath, T. (1989)
ESPRIT-estimation of signal parameters via rotational invariance techniques.
IEEE Transactions on Acoustics, Speech, Signal Processing, **37**, 7 (July 1989), 984–995.

[3] Nehorai, A., and Paldi, E.(1991)
Vector-sensor array processing for electromagnetic source localization.
IEEE Transactions on Signal Processing, **42**, 2 (Feb. 1994), 376–398; and in *Asilomar Conference*, 1991, 566–572.

[4] Li, J. (1993)
Direction and polarization estimation using arrays with small loops and short dipoles.
IEEE Transactions on Antennas and Propagation, **41**, 3 (Mar. 1993), 379–387.

[5] Hochwald, B., and Nehorai, A. (1995)
Polarimetric modeling and parameter estimation with applications to remote sensing.
IEEE Transactions on Signal Processing, **43**, 8 (Aug. 1995), 1923–1935.

[6] Wong, K. T., and Zoltowski, M. D. (1996)
High accuracy 2D angle estimation with extended aperture vector sensor array.
In *Proceedings of International Conference on Acoustics, Speech, Signal Processing*, **5** (1996), 2789–2792.

[7] Zoltowski, M. D., and Wong, K. T. (1997)
Polarization diversity and extended-aperture spatial diversity to mitigate fading-channel effects with a sparse array of electric dipoles or magnetic loops.
In *Proceedings of IEEE International Vehicular Technology Conference*, 1997, 1163–1167.

[8] Wong, K. T., and Zoltowski, M. D. (1997)
Uni-Vector-Sensor ESPRIT for multi-source azimuth, elevation, and polarization estimation.
IEEE Transactions on Antennas and Propagation, **45**, 10 (Oct. 1997), 1467–1474.

[9] Wong, K. T., and Zoltowski, M. D. (1997)
Self-initiating MUSIC-based direction finding in polarization beamspace.
IEE Radar'97 Conference, IEE Publication 449, 328–333.

[10] Wong, K. T. (1998)
Adaptive geolocation and blind beamforming for wideband fast frequency-hop signals of unknown hop sequences and unknown arrival angles using an electromagnetic vector-sensor.
In *Proceedings of IEEE International Conference on Communications*, **2** (1998), 758–762.

[11] Wong, K. T., and Zoltowski, M. D. (1998)
Closed-form direction-finding with arbitrarily spaced electromagnetic vector-sensors at unknown locations.
In *Proceedings of IEEE International Conference on Acoustics, Speech and Signal Processing*, **4** (1998), 1949–1952.

[12] Wong, K. T. (1999)
Geolocation for partially polarized electromagnetic sources using multiple sparsely and uniformly spaced spatially stretched vector sensors.
In *Proceedings of IEEE International Conference on Circuits and Systems*, **3** (1999), 170–174.

[13] Wong, K. T. (1999)
A novel closed-form azimuth/elevation angle and polarization estimation technique using only electric dipole triads or only magnetic loop triads with arbitrary unknown spacings.
In *Proceedings of IEEE International Conference on Circuits and Systems*, **3** (1999), 207–210.

[14] Ho, K.-C., Tan, K.-C., and Nehorai, A. (1999)
Estimating directions of arrival of completely and incompletely polarized signals with electromagnetic vector sensors.
IEEE Transactions on Signal Processing, **47**, 10 (Oct. 1999), 2845–2852.

[15] Nehorai, A., and Tichavsky, P. (1999)
Cross-product algorithms for source tracking using an EM vector sensor.
IEEE Transactions on Signal Processing, **47**, 10 (Oct. 1999), 2863–2867.

[16] Wong, K. T., and Zoltowski, M. D. (2000)
Closed-form direction-finding and polarization estimation with arbitrarily spaced electromagnetic vector-sensors at unknown locations.
IEEE Transactions on Antennas and Propagation, **48**, 5 (May 2000), 671–681.

[17] Zoltowski, M. D., and Wong, K. T. (2000)
ESPRIT-based 2-D direction finding with a sparse uniform array of electromagnetic vector-sensors.
IEEE Transactions on Signal Processing, **48**, 8 (Aug. 2000), 2195–2204.

[18] Zoltowski, M. D., and Wong, K. T. (2000)
Closed-form eigenstructure-based direction finding using arbitrary but identical subarrays on a sparse uniform Cartesian array grid.
IEEE Transactions on Signal Processing, **48**, 8 (Aug. 2000), 2205–2210.

[19] Wong, K. T., and Lai, A. (2000)
Inexpensive upgrade of antenna-switching cellular base-station receivers for uplink/downlink beamforming using a magnetic-loop pair or a loop/dipole triad.
Presented at the *2000 IEEE Global Telecommunications Conference*, 1370–1374.

[20] Wong, K. T., and Zoltowski, M. D. (2000)
Self-initiating MUSIC-based direction finding & polarization estimation in spatio-polarizational beamspace.
IEEE Transactions on Antennas and Propagation, **48**, 9 (Sept. 2000), 1235–1245.

[21] Wong, K. T. (2001)
Geolocation/Beamforming for multiple FFH with unknown hop-sequences.
IEEE Transactions on Aerospace and Electronic Systems, **37**, 1 (Jan. 2001).

Kainam Thomas (Tom) Wong (S'85—M'97—SM'01) earned the B.S.E. (Chem. E.) from U.C.L.A. in 1985, the B.S.E.E. from the University of Colorado, Boulder, in 1987, the M.S.E.E. from the Michigan State University, East Lansing, in 1990, and the Ph.D. in E.E. from Purdue University, West Lafayette, IN in 1996.

Dr. Wong was a Manufacturing Engineer at General Motors Technical Center (Warren, MI) from 1990 to 1991, a Senior Professional Staff Member at The Johns Hopkins University Applied Physics Laboratory (Laurel, MD) from 1996 to 1998, and an Assistant Professor at Singapore's Nanyang Technological University in 1998. He has been an Assistant Professor in the Department of Electronic Engineering at the Chinese University of Hong Kong since 1998. His current interests are signal processing for communications and sensor array signal processing.

Dr. Wong is a contributing author of about 70 articles for the telecommunications section of the inaugural edition (2001) of the CRC Dictionary of Pure and Applied Physics. He serves on the Technical Program Committees of the 1999 and 2000 IEEE Wireless Communications and Networking Conference (WCNC'99, WCNC'00), the 2000 Spring IEEE Vehicular Technology Conference (VTC'00 Spring) and other conferences. He also serves on the Organizing Committees of the 2000 IEEE International Symposium on Circuits and Systems (ISCAS'00) and the Symposium 2000 on Adaptive Signal Processing, Communications and Control (AS-SPCC).